Table III. Bond Distances[a]

Co-O5	2.048 (5)		
O6A-O6B	0.460 (21)		
C1-C2	1.517 (9)		
Co-O1	1.909 (3)	Co-O2	1.901 (3)
Co-N2	1.896 (4)	Co-N1	1.898 (4)
Co-O6A	1.885 (15)	Co-O6B	1.868 (15)
O1-C9	1.308 (6)	O2-C16	1.307 (6)
O5-HX	0.703 (59)	O5-HY	0.848 (70)
N2-C2	1.499 (8)	N1-C1	1.494 (8)
N2-C3	1.279 (7)	N1-C10	1.304 (7)
O3-C8	1.365 (7)	O4-C15	1.351 (7)
O3-C21	1.434 (8)	O4-C22	1.421 (8)
O6A-O7A	1.282 (19)	O6B-O7B	1.223 (19)
C2-C19	1.532 (10)	C1-C17	1.525 (10)
C2-C20	1.551 (11)	C1-C18	1.545 (9)
C3-C4	1.406 (8)	C10-C11	1.407 (8)
C4-C5	1.415 (8)	C11-C12	1.415 (8)
C4-C9	1.415 (8)	C11-C16	1.412 (8)
C5-C6	1.341 (9)	C12-C13	1.334 (9)
C6-C7	1.386 (9)	C13-C14	1.391 (9)
C7-C8	1.372 (8)	C14-C15	1.379 (8)
C8-C9	1.421 (8)	C15-C16	1.421 (8)
C24-C25	1.337 (16)		
O8-C23	1.410 (10)	O9-C25	1.364 (12)
O8-C24	1.416 (13)	O9-C26	1.361 (10)

[a] Distances which were averaged for the discussion are shown side by side.

so as to test this prediction.

Acknowledgment. This work was supported in part by the National Institutes of Health, National Heart, Lung, and Blood Institute (Research Grant No. HL-12395), for which we are grateful. It is a pleasure for us to acknowledge the preliminary work done by Dr. Robert S. Gall on this project. We thank Richard E. Marsh for his continued patient counsel and Sten O. Samson for the construction and maintenance of our X-ray diffraction equipment.

Registry No. Co(3-OMe-Saltmen)$(H_2O)(O_2)\cdot C_4H_{10}O_2$, 68108-70-3; Co(3-OMe-Saltmen), 68108-72-5.

Supplementary Material Available: Table 4 (bond angles), Table 5 (distance and angles in the hydrogen bonding), Table 6 (close nonbonded contacts), Table 7 (residuals in the final difference fourier), and a listing of observed structure factors, their estimated standard deviations, and the calculated structure factors (23 pages). Ordering information is given on any current masthead page.

References and Notes

(1) Previous papers in this series: (1) W. P. Schaefer and R. E. Marsh, *Acta Crystallogr., Sect. B*, **25**, 1675 (1969); (2) B.-C. Wang and W. P. Schaefer, *Science*, **166**, 1404 (1969); (3) L. A. Lindblom, W. P. Schaefer, and R. E. Marsh, *Acta Crystallogr.*, **27**, 1461 (1971); (4) A. Avdeef and W. P. Schaefer, *Inorg. Chem.*, **15**, 1432 (1976); (5) ref 3a; (6) ref 3c; (7) ref 3b; (8) ref 12a.
(2) J. P. Collman, R. R. Gagné, C. A. Reed, W. T. Robinson, and G. S. Rodley, *Proc. Natl. Acad. Sci. U.S.A.*, **71**, 1326–1329 (1974).
(3) (a) R. S. Gall, J. F. Rogers, W. P. Schaefer, and G. G. Christoph, *J. Am. Chem. Soc.*, **98**, 5135–5144 (1976); (b) R. S. Gall and W. P. Schaefer, *Inorg. Chem.*, **15**, 2758–2763 (1976); (c) A. Avdeef and W. P. Schaefer, *J. Am. Chem. Soc.*, **98**, 5153–5159 (1976).
(4) L. Pauling in "Haemoglobin", Butterworths, London, 1949, pp 57–65.
(5) W. A. Goddard, III, and B. D. Olafson, *Proc. Natl. Acad. Sci. U.S.A.*, **72**, 2335–2339 (1975).
(6) R. Sayre, *J. Am. Chem. Soc.*, **78**, 6890 (1956).
(7) W. Busing and H. Levy, *Acta Crystallogr.*, **10**, 180 (1957).
(8) P. Main, M. M. Woolfson, L. Lessinger, G. Germain, and J.-P. Delclercq, "Multan 74", University of York, York, England, and Laboratoire de Chimie Physique et de Cristallographie, Louvain, Belguim, 1974.
(9) $R_1 = \sum||F_o| - |F_c||/\sum F_o$; $R_2 = [\sum w^2(F_o^2 - F_c^2)^2]/\sum w^2F_o^4$. The secondary extinction factor is defined in A. Larson, *Acta Crystallogr.*, **23**, 664 (1967). The goodness of fit = $[\sum w^2(F_o^2 - F_c^2)^2/(n-p)]^{1/2}$; n = the number of data, p = the number of parameters.
(10) Supplementary material.
(11) T. H. Goodwin, M. Przybylska, and J. M. Robertson, *Acta Crystallogr.*, **3**, 279 (1950).
(12) (a) W. P. Schaefer, R. Waltzman, and B. T. Huie, *J. Am. Chem. Soc.*, **100**, 5063 (1978); (b) A. Bigotto, G. Costa, G. Mestroni, G. Pellizer, A. Puxeddu, E. Reisenhofer, L. Stefani, and G. Gaugher, *Inorg. Chim. Acta, Rev.*, **4**, 41 (1970).

Contribution from the Union Carbide Corporation, Chemicals and Plastics, South Charleston, West Virgina 25303

$[Rh_9P(CO)_{21}]^{2-}$. Example of Encapsulation of Phosphorus by Transition-Metal–Carbonyl Clusters

JOSÉ L. VIDAL,* W. E. WALKER, R. L. PRUETT, and R. C. SCHOENING

Received June 23, 1978

The reaction of $Rh(CO)_2$acac with triphenylphosphine in the presence of cesium benzoate in tetraethylene glycol dimethyl ether solution resulted in the selective formation of $[Rh_9P(CO)_{21}]^{2-}$ (80% yield) after 4 h of contact time under ~400 atm of carbon monoxide and hydrogen (CO/H_2 = 1) at 140–160 °C. The cluster has been isolated as the cesium and benzyltriethylammonium salts, both of which are sensitive to moisture and oxygen. The salts are soluble in acetone, acetonitrile, tetrahydrofuran, and sulfolane but insoluble in organic solvents of lower polarity. The $[C_6H_5CH_2N(C_2H_5)_3]_2[Rh_9P(CO)_{21}]\cdot CH_3C(O)CH_3$ complex has been characterized via a complete three-dimensional X-ray diffraction study. The complex crystallizes in the space group $P\bar{1}$ with a = 11.705 (4) Å, b = 12.866 (11) Å, c = 22.747 (12) Å, α = 101.40 (6)°, β = 92.72 (4)°, γ = 108.29 (5)°, V = 3.171 Å^3, and ρ (calcd) = 2.04 g cm^{-3} for mol wt 1952.04 and Z = 2. Diffraction data were collected with an Enraf-Nonius CAD4 automated diffractometer using graphite-monochromatized Mo Kα radiation. The structure was solved by direct methods and refined by difference-Fourier and least-squares techniques. All nonhydrogen atoms have been located and refined; final discrepancy indices are R_F = 4.5% and R_{wF} = 4.7% for 5007 reflections in the range of 0.5° < 2θ < 45°. The anion's structure shows eight rhodium atoms in the corners of a cubic antiprism and the ninth rhodium atom capping one of the square faces, and it also contains a naked phosphorus atom placed near the center of the cluster. Average bonding distances for the anion are in the ranges Rh–Rh = 2.880–3.008 Å, Rh–P = 2.401–3.057 Å, Rh–C = 1.847–2.169 Å, and C–O = 1.153–1.188 Å. ^{13}C and ^{31}P NMR results are interpreted as indicative of the fluxionality of the carbon monoxides and rhodium atom core, respectively. A mechanism is proposed to explain the scrambling of the rhodium atoms.

Introduction

The extreme versatility noted for sulfur ligands has resulted in a large variety of different organometallic species in which the sulfur center is sharing from two to four valence electrons[1] and in complexes in which atomic sulfur acting as a ligand is able to give rise to a large variety of organometallic species, e.g., $S_2Fe_3(CO)_9$,[2] $Co_3(CO)_9S$,[3] and $[Fe_2(CO)_6(\mu\text{-}SCH_3)_2]_2S$.[4] As has been already noted,[1] it might be expected that this

behavior would be paralleled by the adjacent element in the periodic table, phosphorus. A review of the complexes reported as containing coordinated phosphorus species shows that these ligands can donate from two to four electrons, as indicated by the following typical examples: (a) two-electron donor in σ-bonded phosphine and phosphite ligand containing complexes, e.g., $ClRh[P(C_6H_5)_3]_3$,[5] (b) a three-electron donor ligand in $[(CO)_4Mo(\mu\text{-}PET_2)_2Mo(CO)_4]$[6] and in $Co_5(CO)_{11}[P(CH_3)_2]_3$,[7] and (c) a four-electron donor atom in $Ni_8(CO)_8(\mu^4\text{-}PC_6H_5)_6$.[8] In contrast to those containing sulfur, transition-metal complexes showing atomic phosphorus acting as a ligand have been reported only in one instance, $[Co_4(\eta^5\text{-}C_5H_5)_4(P)_4]$.[1] The absence of other examples showing coordinated atomic phosphorus, and of situations in which this atom would share all of its valence electrons, prompted us to look for conditions suitable for the preparation of such complexes in an attempt to extend the parallel between sulfur and phosphorus.

The formation of benzene under hydroformylation conditions, in systems containing triphenylphosphine together with rhodium carbonyl clusters,[9] e.g., $Rh_4(CO)_{12}$ and $Rh_6(CO)_{16}$, indicated the loss of phenyl radicals from triphenylphosphine. The ability of precious transition-metal complexes to cleave the P–C bond present in coordinated arylphosphines[10,11] suggested to us that metalation of these ligands could also occur in the case of clusters, because of the presence of several metal atoms neighboring the bonding site. It was considered probable that successive losses of phenyl radicals from triphenylphosphine could result in "naked" phosphorus coordinated to a rhodium carbonyl cluster, and it was expected that rhodium–carbonyl clusters containing encapsulated atomic phosphorus could be prepared under reaction conditions similar to those previously reported for $[Rh_{17}S_2(CO)_{32}]^{3-}$.[12,13]

We have prepared, isolated, and characterized in this work $[Rh_9P(CO)_{21}]^{2-}$. This cluster contains a phosphorus atom placed inside the cluster's cavity, and it provides an example of the ability of phosphorus to parallel the chemistry previously reported for encapsulated sulfur in $[Rh_{17}S_2(CO)_{32}]^{3-}$. It also illustrates that atomic phosphorus is able to share all of its valence electrons as previously noted for sulfur.[12,13]

Experimental Section

Rhodium dicarbonyl acetylacetonate, cesium benzoate, and triphenylphosphine were obtained from Matthey-Bishop, Strem Chemical Co., and Aldrich Chemical Co., respectively, while tetraethylene glycol dimethyl ether was acquired from Ansul Co. and carbon monoxide and hydrogen were obtained from the Linde Division of Union Carbide. All materials were used as obtained.

The synthesis was conducted in a high-pressure autoclave from Autoclave Engineering, and the system was manipulated with rigorous exclusion of air. Infrared spectra were obtained with a Perkin-Elmer 283 infrared spectrometer. The ^{13}C, ^{1}H, and ^{31}P NMR spectra were taken on a Varian XL-100 Fourier transform spectrometer using a acetone-d_6 solution of the compound. Chemical shifts are reported as ppm downfield of tetramethylsilane and H_3PO_4, both used as external standards. Elemental analysis was conducted by Schwarzkopf Microanalytical Laboratory, Woodside, N.Y. All of the work was done in absence of air, with Schlenk equipment and by use of dried solvents.

Crystals have been obtained by the slow diffusion method using acetone–2-propanol. The crystal and molecular structures were determined by Molecular Structure Corp., College Station, Texas.

Synthesis of $[Rh_9P(CO)_{21}]^{2-}$ Salts. $Rh(CO)_2acac$ (12.0657 g, 46.59 mmol) and cesium benzoate (2.7983 g, 11.02 mmol) were dissolved in 1 L of tetraethylene glycol dimethyl ether. Triphenylphosphine (2.0708 g, 7.87 mmol) was added to the solution and rapid color changes from green-brown to yellow to green and finally to brown were noted. The final solution was charged to a previously evacuated high-pressure autoclave, which was then pressurized to approximately 300 atm with carbon monoxide and hydrogen in 1:1 molar ratio. The temperature was then raised to 140–160 °C and the reaction was allowed to continue overnight, while being stirred. The resulting solution was collected into a 1.5-L Schlenk receiver, after being cooled under pressure to 50 °C. The mixture was filtered and the filtrate was treated with toluene in 10:1 ratio. The solvent was decanted and the resulting oil was redissolved in acetone or in tetrahydrofuran. The filtered extract was then treated with a 2-propanol solution of benzyltriethylammonium chloride (1 g in 15 mL) in 1:1 volume ratio. The solid formed was separated by filtration, washed with fresh 2-propanol, and vacuum-dried. The product (8.03 g) corresponded to a yield of 80% based on the initial rhodium compound. The $[C_6H_5CH_2N(C_2H_5)_3]^+$ salt is soluble in acetone, acetonitrile, dimethyl sulfoxide, and similar solvents but shows either slight solubility or insolubility in less polar solvents. The cesium salt, by contrast, is soluble in the solvents previously mentioned and in methanol, tetrahydrofuran, and 1,4-dioxane as well as in glymes and ether-like solvents. Anal. Calcd for $Rh_9PO_{22}N_2C_{50}H_{50}$: C, 30.19; H, 2.54; N, 1.41; Rh, 46.59; P, 1.56. Found: C, 28.05, 28.03; H, 2.54, 2.58; N, 1.41, 1.51; Rh, 47.00, 47.14; P, 1.37, 1.54.

X-ray Data Collection. A black prismatic crystal with dimensions 0.2 × 0.2 × 0.17 mm was selected for the study. It was mounted on a thin glass fiber which was then inserted into a 0.2-mm glass capillary. The capillary was flame-sealed and seated on a eucentric goniometer. All of the manipulations concerning the crystal were conducted under argon.

The goniometer was mounted on an Enraf-Nonius CAD4 automated diffractometer under the control of a PDP 8a computer coupled to a PDP 11/45 computer. The diffractometer was equipped with a molybdenum X-ray tube [λ(Mo K$\bar{\alpha}$) 0.71073 Å] and a graphite-crystal incident-beam monochromator. The crystal was centered in a random orientation. Intensity data were now collected via a θ–2θ scan, from [2θ(Mo Kα_1) − 0.5] to [2θ(Mo Kα_2) + 0.5] over a data range of $0° < 2\theta(\text{Mo K}\alpha) < 45°$, using the following experimental settings: temperature, 23 °C; crystal-to-detector distance, 21 cm; counter aperture width, 2.0 mm; incident-beam collimator diameter, 2.0 mm; takeoff angle, 2.8°; scan rate of 4–20°/min. The variable scan rate allows rapid data collection for intense reflections where a fast scan rate is used and ensures good counting statistics for weak reflections where a slow scan rate is used. Moving-crystal, moving-counter background counts were taken at each end of the scan range, with the ratio, R, of the scan time to background counting time being 2.0. Three strong representative reflections were measured periodically as a check on crystal and electronic stability of the system. No significant changes were found. The net intensity (I) and its standard deviation ($\sigma(I)$) were calculated from

$$I = S(C - RB)$$

$$\sigma(I) = [S^2(C + R^2B) + (PI)^2]^{1/2}$$

where S is the scan rate, C is the total integrated peak count, R is the ratio of scan time to background counting time, B is the total background count, and the parameter P is a factor introduced to downweight intense reflections. Here P was set to 0.05. Lorentz and polarization corrections were applied to the data but extinction and absorption corrections or a correction for changes in intensity of the standard reflections were not necessary. Two space groups were initially probable, $P1$ or $P\bar{1}$, but data refinement confirmed the space group $P\bar{1}$. Twenty-five reflections were used in the determination of the unit cell dimensions (Figure 1). Numerical information on data collection is given in Table I.

Solution and Refinement of the Structure. The structural analysis was done using the computer programs of the Enraf-Nonius structure determination package on the PDP 11/45 computer system at the Molecular Structure Corp., College Station, Texas.

Scattering factors were taken from Cromer and Waber.[14] Both the real, $\Delta f'$, and imaginary, $\Delta f''$, components of anomalous dispersion were those of Cromer and Liberman.[15] Anomalous dispersion effects were included in F_c.

The function minimized during least-squares refinement was $\sum w(|F_o| - |F_c|)^2$, where the weight w is defined as $4F_o^2/\sigma^2(F_o^2)$. Discrepancy indices used are defined in eq 1 and 2.

$$R_F\ (\%) = \sum||F_o| - |F_c||/\sum|F_o| \times 100 \quad (1)$$

$$R_{wF}\ (\%) = [\sum w(|F_o| - |F_c|)^2/\sum w|F_o|^2]^{1/2} \times 100 \quad (2)$$

The structure was solved by direct methods. A total of 16 phase sets were produced using 404 reflections with $|E_{min}| = 2.00$ and 2000 phase relationships. An E map prepared from the phase set showing

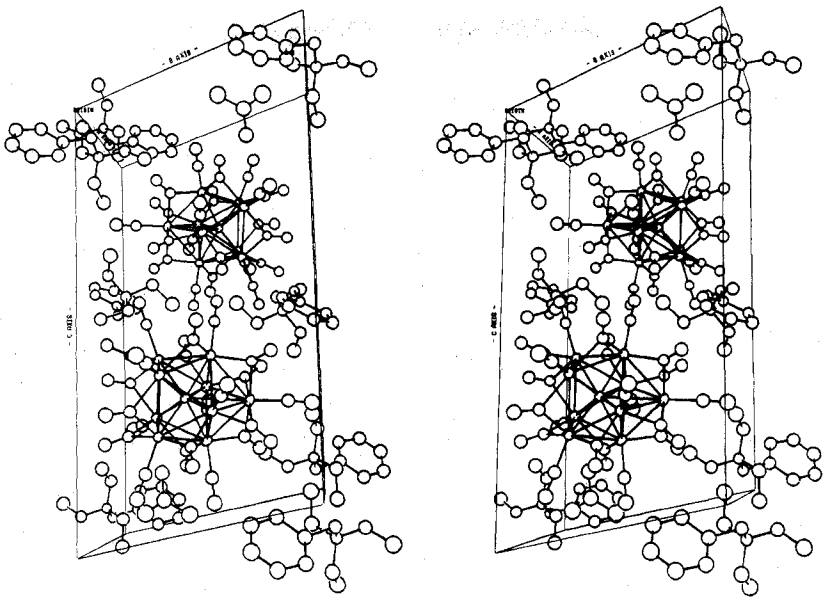

Figure 1. Stereoviews of the unit cell of $[C_6H_5CH_2N(C_2H_5)_3][Rh_9P(CO)_{21}]\cdot CH_3C(O)CH_3$ with the hydrogen atoms omitted.

Table I. Data for the X-ray Diffraction Study of $[C_6H_5CH_2N(C_2H_5)_3]_2[Rh_9P(CO)_{21}]\cdot CH_3C(O)CH_3$

(A) Crystal Data

crystal system: triclinic	$V = 3171$ Å^3
space group: $P\bar{1}$	$T = 23$ °C
$a = 11.705$ (4) Å	$Z = 2$
$b = 12.886$ (11) Å	mol wt = 1952.04
$c = 22.747$ (12) Å	ρ(calcd) = 2.04 g cm^{-3}
$\alpha = 101.40$ (6)°	
$\beta = 92.72$ (4)°	
$\gamma = 108.29$ (5)°	

(B) Intensity Data

radiation	Mo Kα
monochromator	graphite-crystalline incident-beam
reflections measd	$+h, \pm k, \pm l$
max 2θ	45°
min 2θ	0.5°
scan type	θ-2θ
scan speed	4–20°/min
scan range	symmetrical, $[2\theta + \Delta(\alpha_2 - \alpha_1)]$°
reflections collected	8405 total, 8251 independent
linear absorption coeff	23.06 cm^{-1}; no absorption corrections made

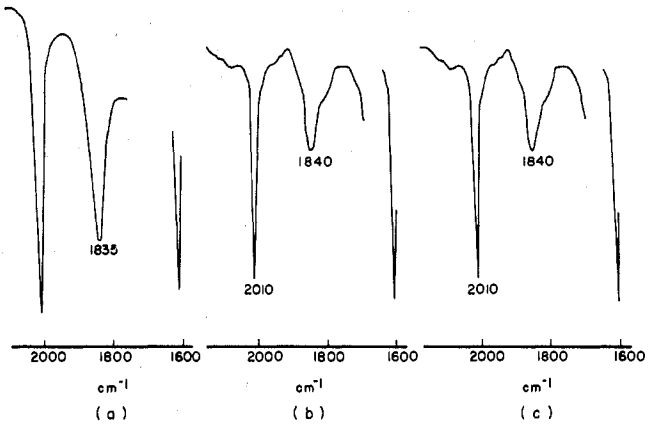

Figure 2. Infrared spectra (wavenumbers ±5 cm^{-1}) of $[Rh_9P(CO)_{21}]^{2-}$ (cesium and benzyltriethylammonium salts): (a) in situ spectrum taken at 4 h after mixing under 300–400 atm of carbon monoxide and hydrogen at 140–160 °C; (b) isolated-product spectrum; (c) spectrum after exposure to 600 atm of carbon monoxide and hydrogen for 4 h at 240–270 °C.

the first best probability statistics (absolute figure of merit = 1.005, residual = 20.86) resulted in a quick determination of the position of the nine rhodium atoms. These atoms were included in full-matrix least-squares refinement resulting in agreement factors of $R_F = 21\%$ and $R_{wF} = 25\%$. A Fourier synthesis then led to the unambiguous location of all remaining nonhydrogen atoms.

The analysis was continued using only 5007 reflections having $|F_o|^2 > 3\sigma(|F_o|^2)$. Refinement of positional and anisotropic thermal parameters for all nonhydrogen atoms led to convergence with $R_F = 4.5\%$ and $R_{wF} = 5.7\%$, for a total of 84 nonhydrogen atoms with a number of variable parameters of 386, resulting in values of 1.58 for the esd of an observation of unit weight and 0.5 esd for the maximum parameter shift. The function $\sum w(|F_o| - |F_c|)^2$ showed no appreciable dependence either upon $\lambda^{-1} \sin\theta$ or upon $|F_o|$, and the weighting scheme is thus acceptable. In addition, the final difference-Fourier map showed no residual electron density as high as carbon atoms on a previous difference-Fourier map, as indicated by a value of 0.96 e/Å^3 for the absolute height of the residual peaks.

A table of observed and calculated structure factor amplitudes is available.[16] Positional parameters are collected in Table II.

Results and Discussion

Triphenylphosphine reacts slowly with $Rh(CO)_2acac$ or with the clusters resulting from the reaction of this complex with alkali carboxylate salts at room temperature, as indicated by infrared studies of the initial mixture. By contrast, a selective and fast reaction is obtained upon treatment of the system under more drastic conditions such as 140–160 °C and ~300–400 atm of carbon monoxide and hydrogen, as indicated by the infrared spectrum of the solution after 3–4 h of contact time (Figure 2a). This infrared pattern is also shown by the isolated cesium and benzyltriethylammonium salts of $[Rh_9P(CO)_{21}]^{2-}$, and the similarity suggests that this anionic cluster is either the only or the main rhodium–carbonyl complex present in the solution.

The presence of a naked phosphorus atom inside the cluster's cavity (vide infra) shows that the loss of the three phenyl radicals of triphenylphosphine has occurred under reaction conditions. It appears that this behavior could be facilitated, or perhaps caused, by the presence of several transition-metal atoms surrounding the coordination site of R_3P as in $Rh_x(CO)_y(PR_3)_z$.[9,18,19] The ability of species like this to metalate the phosphorus ligand could result in the cleavage of the P–C bond involved, as suggested by the behavior of some low-oxidation-state mono- and polynuclear precious metal complexes.[10,11,17]

Some representative examples of the ability of phosphorus to generate a wide number of different bonding and stereo-

Table II. Positional Parameters and Their Estimated Standard Deviations for $[C_6H_5CH_2N(C_2H_5)_3]_2[Rh_9P(CO)_{21}]\cdot CH_3C(O)CH_3$

atom	*x*	*y*	*z*	atom	*x*	*y*	*z*
Rh(1)	0.09330 (9)	0.62454 (8)	0.20734 (4)	C(9)	−0.256 (1)	0.126 (1)	0.2177 (7)
Rh(2)	0.17086 (9)	0.60273 (8)	0.32879 (5)	C(10)	0.232 (1)	0.713 (1)	0.2693 (6)
Rh(3)	−0.04824 (9)	0.64297 (8)	0.37343 (4)	C(11)	0.025 (1)	0.765 (1)	0.2265 (6)
Rh(4)	−0.12335 (9)	0.66963 (8)	0.25316 (5)	C(12)	0.153 (1)	0.484 (1)	0.1707 (6)
Rh(5)	−0.14369 (9)	0.45743 (8)	0.17593 (5)	C(13)	0.145 (1)	0.724 (1)	0.3872 (6)
Rh(6)	0.06994 (9)	0.40860 (8)	0.23023 (5)	C(14)	0.138 (1)	0.467 (1)	0.3814 (6)
Rh(7)	−0.03041 (9)	0.42008 (8)	0.34866 (4)	C(15)	−0.063 (1)	0.772 (1)	0.3421 (6)
Rh(8)	−0.24349 (9)	0.46844 (9)	0.29549 (5)	C(16)	−0.240 (1)	0.553 (1)	0.3755 (6)
Rh(9)	−0.17631 (1)	0.27918 (9)	0.23815 (5)	C(17)	−0.232 (1)	0.560 (1)	0.1681 (6)
P(1)	−0.0357 (3)	0.5304 (3)	0.2758 (1)	C(18)	−0.271 (1)	0.312 (1)	0.1667 (7)
O(1)	0.1680 (10)	0.7015 (9)	0.0947 (5)	C(19)	−0.037 (1)	0.263 (1)	0.1832 (6)
O(2)	0.4344 (11)	0.6437 (11)	0.3645 (5)	C(20)	−0.068 (1)	0.257 (1)	0.3137 (6)
O(3)	−0.0359 (9)	0.7209 (7)	0.5078 (4)	C(21)	−0.309 (1)	0.307 (1)	0.2956 (6)
O(4)	−0.2893 (12)	0.8048 (10)	0.2448 (6)	C(22)	0.313 (2)	−0.053 (1)	0.0453 (8)
O(5)	−0.0947 (11)	0.4258 (9)	0.0460 (5)	C(23)	0.321 (2)	−0.052 (2)	−0.0201 (9)
O(6)	0.2693 (11)	0.3243 (9)	0.2672 (5)	C(24)	0.359 (1)	0.154 (1)	0.0770 (7)
O(7)	−0.1415 (9)	0.4009 (7)	0.4656 (4)	C(25)	0.342 (2)	0.255 (2)	0.1198 (9)
O(8)	−0.4791 (11)	0.4893 (10)	0.2506 (5)	C(26)	0.255 (2)	0.022 (1)	0.1453 (8)
O(9)	−0.3054 (12)	0.0322 (10)	0.2020 (6)	C(27)	0.384 (2)	0.038 (2)	0.1804 (9)
O(10)	0.3206 (10)	0.7939 (9)	0.2735 (5)	C(28)	0.143 (1)	0.038 (1)	0.0529 (7)
O(11)	0.0687 (9)	0.8567 (8)	0.2218 (4)	C(29)	0.040 (1)	−0.073 (1)	0.0552 (7)
O(12)	0.2146 (9)	0.4714 (8)	0.1319 (4)	C(30)	0.017 (2)	−0.176 (1)	0.0057 (8)
O(13)	0.2036 (8)	0.8119 (7)	0.4199 (4)	C(31)	−0.091 (2)	−0.267 (1)	0.0061 (8)
O(14)	0.2074 (9)	0.4451 (8)	0.4126 (4)	C(32)	−0.155 (2)	−0.261 (1)	0.0523 (9)
O(15)	−0.0487 (9)	0.8693 (8)	0.3629 (4)	C(33)	−0.143 (2)	−0.169 (1)	0.0959 (8)
O(16)	−0.3059 (9)	0.5662 (8)	0.4134 (4)	C(34)	−0.042 (1)	−0.071 (1)	0.0997 (7)
O(17)	−0.3074 (9)	0.5703 (8)	0.1365 (5)	C(35)	0.262 (1)	0.182 (1)	0.4794 (7)
O(18)	−0.3632 (10)	0.2576 (8)	0.1344 (3)	C(36)	0.161 (1)	0.073 (1)	0.4874 (7)
O(19)	−0.0344 (9)	0.1895 (8)	0.1414 (4)	C(37)	0.291 (1)	0.077 (1)	0.3769 (7)
O(20)	−0.0472 (9)	0.1785 (7)	0.3238 (4)	C(38)	0.196 (2)	0.112 (2)	0.3439 (9)
O(21)	−0.3921 (9)	0.2427 (8)	0.3114 (4)	C(39)	0.433 (1)	0.264 (1)	0.4208 (7)
O(22)	0.4883 (15)	0.7997 (13)	0.0498 (7)	C(40)	0.497 (2)	0.349 (2)	0.4767 (9)
N(1)	0.270 (1)	0.0419 (8)	0.0815 (5)	C(41)	0.423 (1)	0.095 (1)	0.4675 (6)
N(2)	0.351 (1)	0.1516 (8)	0.4362 (5)	C(42)	0.524 (1)	0.067 (1)	0.4324 (4)
C(1)	0.139 (1)	0.672 (1)	0.1391 (7)	C(43)	0.644 (1)	0.139 (1)	0.4453 (5)
C(2)	0.331 (1)	0.625 (1)	0.3503 (7)	C(44)	0.737 (1)	0.110 (1)	0.4155 (7)
C(3)	−0.044 (1)	0.693 (1)	0.4569 (6)	C(45)	0.707 (1)	0.011 (1)	0.3733 (7)
C(4)	−0.224 (1)	0.753 (1)	0.2477 (7)	C(46)	0.587 (1)	−0.064 (1)	0.3608 (7)
C(5)	−0.112 (1)	0.436 (1)	0.0977 (7)	C(47)	0.496 (1)	−0.038 (1)	0.3904 (6)
C(6)	0.193 (1)	0.358 (1)	0.2525 (6)	C(48)	0.410 (2)	0.601 (2)	0.0219 (11)
C(7)	−0.099 (1)	0.408 (1)	0.4217 (6)	C(49)	0.468 (2)	0.713 (2)	0.0695 (10)
C(8)	−0.390 (1)	0.477 (1)	0.2682 (7)	C(50)	0.483 (2)	0.718 (2)	0.1332 (9)

Chart I

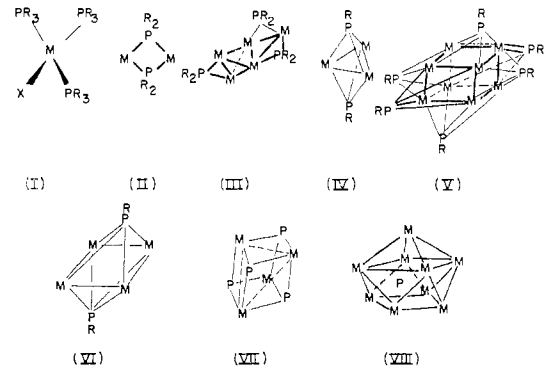

chemical situations are shown in Chart I. A comparison with complexes containing sulfur ligands[1-4,12,13] indicates that although phosphorus is a less versatile ligand than sulfur, it parallels the behavior of the latter element with respect to its ability to coordinate with one or more metal atoms sharing either two (I), three (II–VII), or all of its valence electrons (VIII).

The coordination of *atomic phosphorus* is illustrated in two instances, VII and VIII, in Chart I. In the former compound the phosphorus atom is considered a three-electron donor ligand,[1] while this atom is a five-electron donor ligand in the case of $[Rh_9P(CO)_{21}]^{2-}$ as indicated by the apparent absence of radicals bonded to it and its complete encapsulation inside the cavity of the cluster. This behavior is similar to that of sulfur in $[Rh_{17}S_2(CO)_{32}]^{3-}$.[12,13]

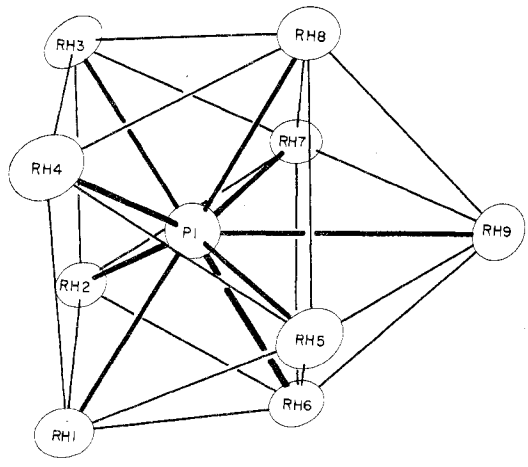

Figure 3. ORTEP diagram of $[Rh_9P(CO)_{21}]^{2-}$ without the carbon monoxide ligands.

Structure of $[Rh_9P(CO)_{21}]^{2-}$ The structure of the anion consists of eight rhodium atoms arranged on the corners of a cubic antiprism, having the ninth rhodium atom capping one of the two square faces (Figure 3). The phosphorus atom is located inside the cavity of the cluster while the carbonyl ligands are distributed with one terminally bonded to each rhodium atom and with three sets of four bridging ligands

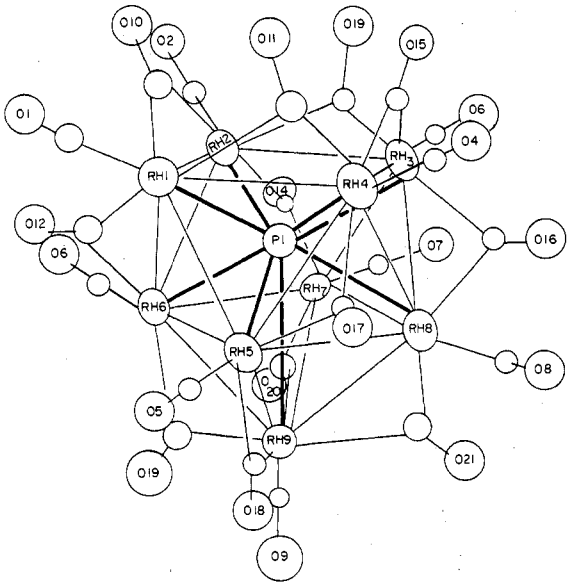

Figure 4. ORTEP diagram of $[Rh_9P(CO)_{21}]^{2-}$ showing the carbon monoxide ligands.

each, bonded between the apical and upper plane metal atoms, the upper and basal plane rhodium atoms, and in between the metal atoms on the basal plane, Figure 4.

Rhodium–rhodium distances are in the range of bonding values previously reported for other rhodium–carbonyl clusters.[20] Average values of 2.880, 2.883, 2.959, and 3.008 Å are detected for the bonds between the apical and upper plane rhodium atoms (Rh(9), Rh(5), Rh(6), Rh(7), Rh(8)), the interplanar rhodium bonds (Rh(1), Rh(2), Rh(3), Rh(4) bonds to Rh(5), Rh(6), Rh(7), Rh(8)), the intraplanar basal (Rh(1), Rh(2), Rh(3), Rh(4)) rhodium–rhodium bonding lengths, and upper plane (Rh(5), Rh(6), Rh(7), Rh(8)) rhodium–rhodium bonding lengths, respectively (Table III).

The latter value is one of the longest bonding distances reported for rhodium–rhodium bonds in clusters.[21] The steric demands of the phosphorus atom could be responsible for this enlargement since the location of this atom on the C_4 axis of symmetry passing through the Rh(9)–P geometric center positions is off from this center and since it is displaced toward the upper plane by about 0.2 Å.

The cluster's phosphorus–rhodium mean distances in the case of the metal atoms placed on the upper and basal planes, 2.401 and 2.449 Å (Table III), are nearly equal to those expected from the sum of the radii of rhodium in clusters, 1.38 Å,[21] and the covalent radii of phosphorus, 1.10 Å.[22] These values are in contrast with M–P distances somewhat shorter than those expected from the sum of the covalent radii of the respective elements, as found, for instance, in $C_6H_5P[Mn(CO)_2C_5H_5]_2$, 2.184 (2) Å,[23] $Co_4(CO)_{10}(\mu^4\text{-}PC_6H_5)_2$[24] with a range of 2.237 (3)–2.255 (3) Å and an average value of 2.244 Å, and $Ni_8(CO)_8(\mu^4\text{-}PC_6H_5)_6$[8] with a range of 2.172 (5)–2.192 (5) Å and a mean value of 2.183 Å. This different behavior could be due to the differences in the hybridization of the phosphorus atom and the phosphorus–metal orbital combinations as suggested in some instances.[24,25] Hence, it is perhaps possible that the absence of groups giving two-electron bonds to phosphorus for the case of the encapsulated element could be responsible for this atom showing size similar to that in the most ideal situation. Finally, the apical rhodium–phosphorus distance of 3.057 (3) Å is longer than that expected for a direct bonding interaction between the two atoms involved.

The structural comparison of rhodium–carbonyl clusters with encapsulated group 5A and 6A elements, $[Rh_9P(CO)_{21}]^{2-}$ and $[Rh_{17}S_2(CO)_{32}]^{3-}$,[12] is tempting based on previous results

Table III. Interatomic Distances and Esd's for $[Rh_9P(CO)_{21}]^{2-}$ (Å)[a]

(a) Rhodium–Rhodium and Rhodium–Phosphorus Distances

Rh(1)–Rh(2)	2.961 (1)	Rh(6)–Rh(7)	2.985 (1)
Rh(1)–Rh(4)	2.965 (1)	Rh(6)–Rh(9)	2.876 (1)
Rh(1)–Rh(5)	2.880 (1)	Rh(7)–Rh(8)	3.010 (1)
Rh(1)–Rh(6)	2.863 (1)	Rh(7)–Rh(9)	2.894 (1)
Rh(2)–Rh(3)	2.958 (1)	Rh(8)–Rh(9)	2.883 (1)
Rh(2)–Rh(6)	2.891 (1)	Rh(1)–P(1)	2.449 (3)
Rh(2)–Rh(7)	2.887 (1)	Rh(2)–P(1)	2.457 (3)
Rh(3)–Rh(4)	2.951 (1)	Rh(3)–P(1)	2.439 (3)
Rh(3)–Rh(7)	2.891 (1)	Rh(4)–P(1)	2.451 (3)
Rh(3)–Rh(8)	2.870 (1)	Rh(5)–P(1)	2.404 (3)
Rh(4)–Rh(5)	2.876 (1)	Rh(6)–P(1)	2.400 (3)
Rh(4)–Rh(8)	2.907 (1)	Rh(7)–P(1)	2.397 (3)
Rh(5)–Rh(6)	3.029 (1)	Rh(8)–P(1)	2.404 (3)
Rh(5)–Rh(8)	3.006 (1)	Rh(9)–P(1)	3.057 (3)
Rh(5)–Rh(9)	2.865 (1)		

(b) Rhodium–Carbon Distances

Terminal Carbonyls

Rh(1)–C(1)	1.820 (13)	Rh(6)–C(6)	1.849 (13)
Rh(2)–C(2)	1.833 (14)	Rh(7)–C(7)	1.891 (12)
Rh(3)–C(3)	1.874 (12)	Rh(8)–C(8)	1.845 (15)
Rh(4)–C(4)	1.845 (15)	Rh(9)–C(9)	1.847 (14)
Rh(5)–C(5)	1.822 (14)		

Bridge Carbonyls

Rh(1)–C(10)	1.975 (2)	Rh(5)–C(17)	1.942 (12)
Rh(1)–C(11)	2.176 (12)	Rh(5)–C(18)	1.962 (13)
Rh(1)–C(12)	2.173 (12)	Rh(6)–C(12)	1.940 (11)
Rh(2)–C(10)	2.140 (12)	Rh(6)–C(19)	1.959 (12)
Rh(2)–C(13)	1.957 (11)	Rh(7)–C(14)	1.933 (12)
Rh(2)–C(14)	2.251 (11)	Rh(7)–C(20)	1.996 (11)
Rh(3)–C(13)	2.150 (11)	Rh(8)–C(16)	1.920 (12)
Rh(3)–C(15)	1.989 (11)	Rh(8)–C(21)	1.978 (11)
Rh(3)–C(16)	2.191 (12)	Rh(9)–C(18)	2.110 (13)
Rh(4)–C(11)	1.983 (12)	Rh(9)–C(19)	2.138 (12)
Rh(4)–C(15)	2.136 (11)	Rh(9)–C(20)	2.207 (11)
Rh(4)–C(17)	2.214 (12)	Rh(9)–C(21)	2.146 (11)

(c) Carbon–Oxygen Distances

Terminal Carbonyls

C(1)–O(1)	1.177 (13)	C(6)–O(6)	1.166 (14)
C(2)–O(2)	1.171 (15)	C(7)–O(7)	1.145 (12)
C(3)–O(3)	1.132 (12)	C(8)–O(8)	1.161 (15)
C(4)–O(4)	1.165 (15)	C(9)–O(9)	1.141 (14)
C(5)–O(5)	1.189 (14)		

Bridge Carbonyls

C(10)–O(10)	1.195 (13)	C(16)–O(16)	1.204 (13)
C(11)–O(11)	1.163 (12)	C(17)–O(17)	1.170 (13)
C(12)–O(12)	1.186 (12)	C(18)–O(18)	1.197 (14)
C(13)–O(13)	1.197 (11)	C(19)–O(19)	1.212 (13)
C(14)–O(14)	1.192 (12)	C(20)–O(20)	1.168 (11)
C(15)–O(15)	1.200 (12)	C(21)–O(21)	1.187 (12)

[a] A complete set of bonding distances for $[C_6H_5CH_2N(C_2H_5)_3]_2[Rh_9P(CO)_{21}]\cdot CH_3C(O)CH_3$, including the distances for the cation and the solvate acetone molecule, is available as supplementary material.

discussed for $Co_4(CO)_{10}(\mu^4\text{-}X)_2$ (X = PC_6H_5, S), although it should be kept in mind that the uncertainties introduced by comparison of clusters of formally nonequivalent structures could lead to erroneous conclusions.[24] Once that is recognized, a restricted structural comparison between $[Rh_9P(CO)_{21}]^{2-}$ and $[Rh_{17}S_2(CO)_{32}]^{3-}$ is reasonable, if the attention is limited to the M_4E moieties corresponding to the basal planes and the variation of some structural parameters is considered upon formal substitution of phosphorus for sulfur in $Co_4(CO)_8(\mu^4\text{-}X)$, $[Rh_9P(CO)_{21}]^{2-}$, and $[Rh_{17}S_2(CO)_{21}]^{3-}$. Thus, while the M–M distance increases by 0.04 Å in the cobalt complexes, a similar increase of 0.08 Å is detected for the rhodium clusters. By contrast, an increase of ca. 1.8° is noted for the M–E–M angle in the former series, but one of 3.4° is found

Table IV. Angles with Esd's within $[Rh_9P(CO)_{21}]^{2-}$ (deg)[a]

(a) Rhodium–Rhodium–Rhodium Groups

Rh(2)–Rh(1)–Rh(4)	89.66 (3)	Rh(1)–Rh(6)–Rh(5)	58.44 (3)	Rh(1)–Rh(4)–Rh(3)	90.20 (3)	Rh(8)–Rh(7)–Rh(9)	58.42 (3)
Rh(2)–Rh(1)–Rh(5)	103.48 (3)	Rh(1)–Rh(6)–Rh(7)	102.36 (3)	Rh(1)–Rh(4)–Rh(5)	59.07 (3)	Rh(3)–Rh(8)–Rh(4)	61.43 (3)
Rh(2)–Rh(1)–Rh(6)	59.49 (3)	Rh(1)–Rh(6)–Rh(9)	112.91 (4)	Rh(1)–Rh(4)–Rh(8)	102.49 (4)	Rh(3)–Rh(8)–Rh(5)	101.63 (4)
Rh(4)–Rh(1)–Rh(5)	58.93 (3)	Rh(2)–Rh(6)–Rh(5)	101.54 (3)	Rh(3)–Rh(4)–Rh(5)	102.89 (4)	Rh(3)–Rh(8)–Rh(7)	58.84 (3)
Rh(4)–Rh(1)–Rh(6)	103.32 (3)	Rh(2)–Rh(6)–Rh(7)	58.83 (3)	Rh(3)–Rh(4)–Rh(8)	58.66 (3)	Rh(3)–Rh(8)–Rh(9)	113.47 (4)
Rh(5)–Rh(1)–Rh(6)	63.67 (3)	Rh(2)–Rh(6)–Rh(9)	113.72 (4)	Rh(5)–Rh(4)–Rh(8)	62.62 (3)	Rh(4)–Rh(8)–Rh(5)	58.18 (3)
Rh(1)–Rh(2)–Rh(3)	90.15 (3)	Rh(5)–Rh(6)–Rh(7)	89.98 (3)	Rh(1)–Rh(5)–Rh(4)	62.01 (3)	Rh(4)–Rh(8)–Rh(7)	101.42 (4)
Rh(1)–Rh(2)–Rh(6)	58.57 (3)	Rh(5)–Rh(6)–Rh(9)	57.98 (3)	Rh(1)–Rh(5)–Rh(6)	57.89 (3)	Rh(4)–Rh(8)–Rh(9)	112.42 (4)
Rh(1)–Rh(2)–Rh(7)	102.39 (3)	Rh(7)–Rh(6)–Rh(9)	59.14 (3)	Rh(1)–Rh(5)–Rh(8)	102.15 (3)	Rh(5)–Rh(8)–Rh(7)	89.96 (3)
Rh(3)–Rh(2)–Rh(6)	102.49 (3)	Rh(2)–Rh(7)–Rh(3)	61.59 (3)	Rh(1)–Rh(5)–Rh(9)	112.72 (4)	Rh(5)–Rh(8)–Rh(9)	58.19 (3)
Rh(3)–Rh(2)–Rh(7)	59.27 (3)	Rh(2)–Rh(7)–Rh(6)	58.95 (3)	Rh(4)–Rh(5)–Rh(6)	101.43 (3)	Rh(7)–Rh(8)–Rh(9)	58.78 (3)
Rh(6)–Rh(2)–Rh(7)	62.22 (3)	Rh(2)–Rh(7)–Rh(8)	101.83 (4)	Rh(4)–Rh(5)–Rh(8)	59.20 (3)	Rh(5)–Rh(9)–Rh(6)	63.69 (3)
Rh(2)–Rh(3)–Rh(4)	89.98 (3)	Rh(2)–Rh(7)–Rh(9)	113.30 (4)	Rh(4)–Rh(5)–Rh(9)	113.89 (4)	Rh(5)–Rh(9)–Rh(7)	95.18 (3)
Rh(2)–Rh(3)–Rh(7)	59.14 (3)	Rh(3)–Rh(7)–Rh(6)	101.82 (4)	Rh(6)–Rh(5)–Rh(8)	89.65 (3)	Rh(6)–Rh(9)–Rh(7)	62.31 (3)
Rh(2)–Rh(3)–Rh(8)	103.52 (3)	Rh(3)–Rh(7)–Rh(8)	58.16 (3)	Rh(6)–Rh(5)–Rh(9)	58.33 (3)	Rh(6)–Rh(9)–Rh(8)	95.24 (3)
Rh(4)–Rh(3)–Rh(7)	103.25 (3)	Rh(3)–Rh(7)–Rh(9)	112.54 (4)	Rh(8)–Rh(5)–Rh(9)	58.76 (3)	Rh(7)–Rh(9)–Rh(8)	62.80 (3)
Rh(4)–Rh(3)–Rh(8)	59.91 (3)	Rh(6)–Rh(7)–Rh(8)	90.41 (3)	Rh(1)–Rh(6)–Rh(2)	61.94 (3)		
Rh(7)–Rh(3)–Rh(8)	62.99 (3)	Rh(6)–Rh(7)–Rh(9)	58.56 (3)				

(b) Angles Involving the P Atom

Rh(2)–Rh(1)–P(1)	52.99 (7)	Rh(1)–Rh(6)–P(1)	54.60 (7)	Rh(9)–Rh(5)–P(1)	70.29 (7)		
Rh(4)–Rh(1)–P(1)	52.80 (7)	Rh(2)–Rh(6)–P(1)	54.38 (7)	Rh(1)–P(1)–Rh(2)	74.25 (8)	Rh(3)–P(1)–Rh(7)	73.40 (8)
Rh(5)–Rh(1)–P(1)	52.87 (7)	Rh(5)–Rh(6)–P(1)	50.95 (7)	Rh(1)–P(1)–Rh(3)	118.0 (1)	Rh(3)–P(1)–Rh(8)	72.68 (8)
Rh(6)–Rh(1)–P(1)	53.04 (7)	Rh(7)–Rh(6)–P(1)	51.48 (7)	Rh(1)–P(1)–Rh(4)	74.47 (8)	Rh(3)–P(1)–Rh(9)	121.7 (1)
Rh(1)–Rh(2)–P(1)	52.76 (7)	Rh(9)–Rh(6)–P(1)	70.14 (7)	Rh(1)–P(1)–Rh(5)	72.81 (8)	Rh(4)–P(1)–Rh(5)	72.65 (8)
Rh(3)–Rh(2)–P(1)	52.56 (6)	Rh(2)–Rh(7)–P(1)	54.45 (7)	Rh(1)–P(1)–Rh(6)	72.36 (8)	Rh(4)–P(1)–Rh(6)	140.9 (1)
Rh(6)–Rh(2)–P(1)	52.59 (6)	Rh(3)–Rh(7)–P(1)	53.96 (7)	Rh(1)–P(1)–Rh(7)	140.2 (1)	Rh(4)–P(1)–Rh(7)	141.7 (1)
Rh(7)–Rh(2)–P(1)	52.57 (7)	Rh(6)–Rh(7)–P(1)	51.57 (7)	Rh(1)–P(1)–Rh(8)	141.4 (1)	Rh(4)–P(1)–Rh(8)	73.57 (8)
Rh(2)–Rh(3)–P(1)	53.10 (7)	Rh(8)–Rh(7)–P(1)	51.27 (7)	Rh(1)–P(1)–Rh(9)	120.2 (1)	Rh(4)–P(1)–Rh(9)	121.4 (1)
Rh(7)–Rh(3)–P(1)	52.64 (7)	Rh(9)–Rh(7)–P(1)	69.85 (7)	Rh(2)–P(1)–Rh(3)	74.34 (8)	Rh(5)–P(1)–Rh(6)	78.18 (8)
Rh(8)–Rh(3)–P(1)	53.09 (7)	Rh(3)–Rh(8)–P(1)	54.23 (7)	Rh(2)–P(1)–Rh(4)	116.7 (1)	Rh(5)–P(1)–Rh(7)	124.7 (1)
Rh(1)–Rh(4)–P(1)	52.73 (7)	Rh(4)–Rh(8)–P(1)	53.97 (7)	Rh(2)–P(1)–Rh(5)	141.4 (1)	Rh(5)–P(1)–Rh(8)	77.40 (9)
Rh(3)–Rh(4)–P(1)	52.70 (6)	Rh(5)–Rh(8)–P(1)	51.30 (7)	Rh(2)–P(1)–Rh(6)	73.04 (8)	Rh(5)–P(1)–Rh(9)	61.95 (6)
Rh(5)–Rh(4)–P(1)	52.91 (7)	Rh(7)–Rh(8)–P(1)	51.09 (7)	Rh(2)–P(1)–Rh(7)	72.98 (8)	Rh(6)–P(1)–Rh(7)	76.95 (9)
Rh(8)–Rh(4)–P(1)	52.47 (7)	Rh(9)–Rh(8)–P(1)	69.98 (7)	Rh(2)–P(1)–Rh(8)	140.7 (1)	Rh(6)–P(1)–Rh(8)	124.6 (1)
Rh(1)–Rh(5)–P(1)	54.32 (7)	Rh(5)–Rh(9)–P(1)	47.76 (5)	Rh(2)–P(1)–Rh(9)	121.9 (1)	Rh(6)–P(1)–Rh(9)	62.25 (6)
Rh(4)–Rh(5)–P(1)	54.44 (7)	Rh(6)–Rh(9)–P(1)	47.61 (5)	Rh(3)–P(1)–Rh(4)	74.23 (8)	Rh(7)–P(1)–Rh(8)	77.64 (8)
Rh(6)–Rh(5)–P(1)	50.86 (7)	Rh(7)–Rh(9)–P(1)	47.42 (5)	Rh(3)–P(1)–Rh(5)	140.3 (1)	Rh(7)–P(1)–Rh(9)	62.72 (7)
Rh(8)–Rh(5)–P(1)	51.30 (7)	Rh(8)–Rh(9)–P(1)	47.63 (5)	Rh(3)–P(1)–Rh(6)	140.9 (1)	Rh(8)–P(1)–Rh(9)	62.39 (7)

(c) Angles Involving Carbon Monoxide Ligands

Rhodium–Terminal Carbonyls

Rh(1)–C(1)–O(1)	179 (1)	Rh(6)–C(6)–O(6)	179 (1)	Rh(4)–C(4)–O(4)	179 (1)	Rh(9)–C(9)–O(9)	177 (1)
Rh(2)–C(2)–O(2)	178 (1)	Rh(7)–C(7)–O(7)	179 (1)	Rh(5)–C(5)–O(5)	176 (1)		
Rh(3)–C(3)–O(3)	176 (1)	Rh(8)–C(8)–O(8)	176 (1)				

Rhodium–Bridge Carbonyls

Rh(1)–C(10)–O(10)	137 (1)	Rh(3)–C(16)–O(16)	130 (1)	Rh(2)–C(13)–O(13)	138.7 (9)	Rh(6)–C(19)–O(19)	139 (1)
Rh(2)–C(10)–O(10)	131 (1)	Rh(8)–C(16)–O(16)	141 (1)	Rh(3)–C(13)–O(13)	129.3 (9)	Rh(9)–C(19)–O(19)	132 (1)
Rh(1)–C(11)–O(11)	129 (2)	Rh(4)–C(17)–O(17)	131 (1)	Rh(2)–C(14)–O(14)	130.1 (9)	Rh(7)–C(20)–O(20)	140.7 (9)
Rh(4)–C(11)–O(11)	140 (1)	Rh(5)–C(17)–O(17)	141 (1)	Rh(7)–C(14)–O(14)	143 (1)	Rh(9)–C(20)–O(20)	132.4 (9)
Rh(1)–C(12)–O(12)	131.0 (9)	Rh(5)–C(18)–O(18)	138 (1)	Rh(3)–C(15)–O(15)	136.4 (9)	Rh(8)–C(21)–O(21)	140 (1)
Rh(6)–C(12)–O(12)	141 (1)	Rh(9)–C(18)–O(18)	132 (1)	Rh(4)–C(15)–O(15)	132.3 (9)	Rh(9)–C(21)–O(21)	130.8 (9)

Rhodium–Carbon–Rhodium Groups

Rh(1)–C(10)–Rh(2)	91.9 (5)	Rh(3)–C(16)–Rh(8)	88.3 (5)	Rh(2)–C(13)–Rh(3)	92.0 (4)	Rh(6)–C(19)–Rh(9)	89.1 (5)
Rh(1)–C(11)–Rh(4)	90.8 (5)	Rh(4)–C(17)–Rh(5)	87.3 (5)	Rh(2)–C(14)–Rh(7)	86.9 (5)	Rh(7)–C(20)–Rh(9)	86.9 (4)
Rh(1)–C(12)–Rh(6)	88.0 (5)	Rh(5)–C(18)–Rh(9)	89.4 (5)	Rh(3)–C(15)–Rh(4)	91.3 (4)	Rh(8)–C(21)–Rh(9)	88.6 (4)

[a] Tables including the complete sets of angles for $[C_6H_5CH_2N(C_2H_5)_3]_2[Rh_9P(CO)_{21}]\cdot CH_3C(O)CH_3$ are supplied as supplementary material.

for the two latter complexes. Finally, similar comparison for the M–E distance shows it to be independent of the nature of E (E = P, S) for the Co_4E compounds and to increase by about 0.12 Å in the case of the clusters with encapsulated E atoms. The relative small steric differences between phosphorus and sulfur has precluded a rationalization of the structural changes noted for the Co_4E clusters above, based on size–volume considerations exclusively.[25] By contrast, it appears that steric effects should be more important when the main-element atoms are encapsulated by the cluster, and thus the different structural trends noted for the two series above could be at least partially ascribed to the partial and complete encapsulation of E by the cobalt and rhodium clusters above, respectively.

Rhodium–carbon distances are given in Table III. Comparison of these lengths for the terminal carbonyls of $[Rh_9P(CO)_{21}]^{2-}$ with those previously reported for similar ligands bonded to transition-metal clusters[20] shows that the specific (apical, 1.847 (14) Å; average upper plane, 1.851 Å; average basal plane, 1.843 Å) and the overall average (1.847 Å) values for the anion are within the literature range. A more characteristic situation is present for the bridging carbonyls. In these cases, the differences between the average longer and shorter rhodium–carbon lengths found for each of the three

types of bridging carbonyls (apical: 2.150 and 1.970 Å; inter upper basal planes: 2.207 and 1.934 Å; basal: 2.179 and 1.976 Å) clearly establish these ligands as asymmetric bridges, with the degree of asymmetry being larger for the interplanar ligands, Δ(Rh–C) = 0.273 Å, than for any of the other two kinds of bridges, Δ(Rh–C) = 0.203 and 0.180 Å. In any case, the overall average values for these distances, 2.179 and 1.960 Å, are in the range usually reported for these clusters,[20] although the former length resembles more those found for face-bridging carbonyls than for edge-bridging carbonyl.

Similar asymmetric carbonyl bridges have been found in other clusters,[26] and it is considered that the asymmetric character of these ligands could explain the ready carbonyl mobility noted for the anion (vide infra), since the solid-state structure could be considered as an instantaneous view of the low-energy bending modes that may be involved in some instances in carbonyl scrambling.[26,27]

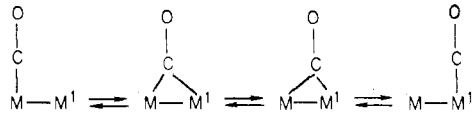

The structure of the anion shows some crowding by the carbonyl ligands as indicated by average carbon–carbon contacts in the range of 2.6–3.0 Å (C(apical terminal)–C(apical bridge) and C(basal terminal)–C(basal bridge), 2.63; C(basal terminal)–C(interplanar bridge), C(apical bridge)–C(apical bridge), and C(upper plane terminal)–C(interplanar bridge), 3.00 Å). These close carbonyl interactions and the long rhodium–rhodium distances present in the structure of $[Rh_9P(CO)_{21}]^{2-}$ could be indicative of cluster instability. In spite of that, the anion seems to be stable under 600–800 atm of carbon monoxide and hydrogen at 140–230 °C, as suggested by the persistence of its characteristic infrared pattern after several hours under these conditions (Figure 2c). Since the only two exceptions to the known transformation of rhodium–carbonyl clusters into $[Rh_{12}(CO)_{34}]^{2-}$ under the above conditions also show encapsulated main-element atoms,[28] $[Rh_6(CO)_{15}C]^{2-}$ and $[Rh_{17}S_2(CO)_{32}]^{3-}$, it is proposed that the high stability of these clusters and of $[Rh_9P(CO)_{21}]^{2-}$ results from the ability of the encapsulated main-element atoms to donate their valence electrons while precluding the destabilization that would result from the steric demands of other ligands, as previously discussed for $[Rh_{15}C_2(CO)_{28}]^-$.[29]

Another structural parallel between $[Rh_9P(CO)_{21}]^{2-}$ and $[Rh_{17}S_2(CO)_{32}]^{3-}$ is the persistence of the preference of the antiprismatic cubic arrangement of metal atoms over the cubic one. Although the reasons for this preference are not obvious because of the potential ability of both conformations to accommodate encapsulated atoms of radii equal to or larger than 1.00 Å,[20] it appears that the presence of four more rhodium–rhodium bonds in the resulting structure could provide the required driving force for its formation. Nevertheless, the different metal skeleton found for other clusters containing encapsulated atoms of radii larger than 1.00 Å, e.g., $[Rh_{13}(CO)_{24}H_3]^{2-}$,[20] indicates that electronic and orbital aspects should also be considered in determining the preferred packing, as already suggested.[21]

Nuclear Magnetic Resonance. The solution structure of $[Rh_9P(CO)_{21}]^{2-}$ was studied by ^1H, ^{13}C, and ^{31}P NMR spectroscopy[30] in an attempt to confirm the persistence of its solid-state structure. The lack of proton resonances in the ^1H NMR spectra, other than those of the cation and the solvating acetone, is consistent with the absence of proton-containing moieties, but further conclusions about the solution structure by means of ^{13}C NMR were precluded by carbonyl fluxionality in the range of temperature tested. In these cases, the only spectral feature corresponding to coordinated carbonyl ligands is a broad resonance band at 210 ppm.

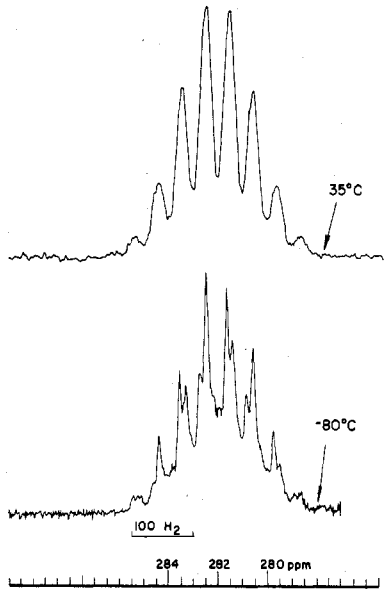

Figure 5. ^{31}P NMR spectra of $[Rh_9P(CO)_{21}]^{2-}$ in acetone-d_6 solution.

In contrast, more relevant structural information was obtained in the case of ^{31}P NMR studies. These spectra demonstrate the presence of a ten-line multiplet centered at 282.3 ppm[30] (Figure 5) and an increase in the multiplicity of the pattern upon decreasing the temperature from +40 to −80 °C. We suggest that fluxionality of the rhodium skeleton could account for these results because thermal averaging of the positions of the rhodium atoms would lead to magnetic equivalence of the nine rhodium and to the observed ten-line pattern (rhodium spin number = $^1/_2$), while a more complex pattern would obviously result from the loss of magnetic equivalence. An alternate possibility such as a change in the solution structure of the anion can be discounted on the basis of the similarities between the infrared spectra in Nujol mull and in solution. An example of the mechanism proposed for this behavior is provided by the rearrangement of a pseudorhombic face, such as the one defined by Rh(9), Rh(7), Rh(8), and Rh(3), into a square face as the basal plane of the solid-state structure achieved mainly by the cleavage of the Rh(7)–Rh(8) bond. The concurrent formation of another rhodium–rhodium bond along the basal square diagonal going through Rh(2) and Rh(4) followed by adequate adjustment of the remaining rhodium–rhodium lengths results in a rhodium skeleton equivalent to the initial one, but with Rh(3) in its apical position. Extension of this mechanism to the remaining faces should result in complete scrambling of the rhodium atoms and in elongation–contraction sequences of each rhodium–rhodium bond giving a "cluster-breathing" movement.[31] A parallel reorganization of the carbonyl ligands required to maintain the initial ligand distribution should then give the observed carbonyl scrambling.

The fluxional behavior of $[Rh_9P(CO)_{21}]^{2-}$ could have a precedent in the partial scrambling of the metal core reported for $[Pt_9(CO)_{18}]^{2-}$[32] and also in the mobility of the iron triangle of $Fe_3(CO)_{12}$[33] inside of a fixed polyhedron formed by the carbonyl ligands. The fluxionality of the former anion could be described in a similar way by a mobile polyhedron of metal atoms circumscribed into a polyhedron described by the oxygen of the carbon monoxide ligands.

Finally, it is noted that the chemical shift for the phosphorus atom in $[Rh_9P(CO)_{21}]^{2-}$ is the farthest downfield resonance detected for this element that we are aware of, and it is indicative of a highly deshielded phosphorus atom.

In addition, the anion has been found to be an exception to the 18-electron rule but it has the number of electrons expected for a nido cluster based on Wade's rules.[34]

Acknowledgment. We appreciate the authorization for publication of this work extended by Union Carbide Corp. We also acknowledge the discussions and suggestions by Professor P. Chini, of the University of Milan, Italy.

Registry No. $[C_6H_5CH_2N(C_2H_5)_3]_2[Rh_9P(CO)_{21}]\cdot CH_3C(O)CH_3$, 68568-12-7; $Cs_2[Rh_9P(CO)_{21}]$, 68408-40-2; $Rh(CO)_2acac$, 14874-82-9; triphenylphosphine, 603-35-0.

Supplementary Material Available: Complete tables of structural factors, atomic distances and angles, and positional and thermal parameters (34 pages). Ordering information is given on any current masthead page.

References and Notes

(1) G. L. Simon and L. F. Dahl, *J. Am. Chem. Soc.*, **95**, 2175 (1973).
(2) C. H. Wei and L. F. Dahl, *Inorg. Chem.*, **4**, 493 (1965).
(3) C. H. Wei and L. F. Dahl, *Inorg. Chem.*, **6**, 1229 (1967).
(4) J. M. Coleman, A. Wojcicki, P. J. Pollick, and L. F. Dahl, *Inorg. Chem.*, **6**, 1936 (1967).
(5) J. A. Osborn, F. H. Jardine, J. F. Young, and G. Wilkinson, *J. Chem. Soc. A*, 1711 (1966).
(6) M. Basato, *J. Chem. Soc., Dalton Trans.*, 1678 (1976).
(7) E. Keller and H. Vahrenkamp, *Angew. Chem., Int. Ed. Engl.*, **16**, 731 (1977).
(8) L. D. Lower and L. F. Dahl, *J. Am. Chem. Soc.*, **98**, 5046 (1976).
(9) P. Chini, S. Martinengo, and G. Garlaschelli, *J. Chem. Soc., Chem. Commun.*, 709 (1972).
(10) H. A. Patel, R. G. Fisher, A. J. Carty, D. V. Naik, and G. J. Palenik, *J. Organomet. Chem.*, **60**, C49 (1973).
(11) W. R. Cullen, D. A. Harbourne, B. V. Liengme, and J. R. Sams, *Inorg. Chem.*, **9**, 702 (1970).
(12) J. L. Vidal, R. A. Fiato, L. A. Cosby, and R. L. Pruett, *Inorg. Chem.*, **17**, 2574 (1978).
(13) J. L. Vidal, R. A. Fiato, L. A. Cosby, and R. L. Pruett, 9th Regional Meeting of the American Chemical Society, Charleston, W.Va., October 1977.
(14) D. T. Cromer and J. T. Waber, "International Tables for X-Ray Crystallography", Vol. IV, in preparation.
(15) D. T. Cromer and D. Liberman, *J. Chem. Phys.*, **53**, 1891 (1970).
(16) Complete structural data for $[C_6H_5CH_2N(C_2H_5)_3][Rh_9P(CO)_{21}]\cdot C_3H_3C(O)CH_3$ is available as supplementary material.
(17) N. J. Taylor, P. C. Chieh, and A. J. Carty, *J. Chem. Soc., Chem. Commun.*, 448 (1975).
(18) B. L. Booth, M. J. Else, R. Fields, and R. N. Haszeldine, *J. Organomet. Chem.*, **27**, 115 (1970).
(19) G. Ciani, L. Garlaschelli, M. Manissero, V. Sartorelli, and V. G. Albano, *J. Organomet. Chem.*, **129**, C25 (1977).
(20) P. Chini, G. Longoni, and V. G. Albano, *Adv. Organomet. Chem.*, **14**, 285.
(21) V. G. Albano, M. Sansoni, P. Chini, and S. Mortinengo, *J. Chem. Soc., Dalton Trans.*, 651 (1973).
(22) L. Pauling, "Nature of the Chemical Bond", 3rd ed., Cornell University Press, Ithaca, N.Y., 1960, p 224.
(23) G. Hutter, H. D. Müller, A. Frank, and H. Lorenz, *Angew. Chem., Int. Ed. Engl.*, **14**, 705 (1975).
(24) R. C. Ryan and L. F. Dahl, *J. Am. Chem. Soc.*, **97**, 6904 (1975).
(25) G. L. Simon and L. F. Dahl, *J. Am. Chem. Soc.*, **95**, 2164 (1973).
(26) P. Chini, *Inorg. Chim. Acta, Rev.*, **2**, 31 (1968).
(27) F. A. Cotton, *Inorg. Chem.*, **5**, 1083 (1966).
(28) J. L. Vidal, D. R. Bryant, R. L. Pruett, L. A. Cosby, and W. E. Walker, 9th Regional Meeting of the American Chemical Society, Charleston, W.Va., October 1977.
(29) V. A. Albano, M. Sansoni, P. Chini, S. Martinengo, and D. Strumolo, *J. Chem. Soc., Dalton Trans.*, 970 (1976).
(30) ^1H, ^{13}C, and ^{31}P NMR studies were conducted with a solution of $[C_6H_5CH_2N(C_2H_5)_3][Rh_9P(CO)_{21}]\cdot CH_3C(O)CH_3$ (1.2 g) in acetone-d_6 (3 mL) or acetonitrile-d_3. This solution was enriched with 90% ^{13}C carbon monoxide at 25 °C under 1 atm of pressure. ^1H NMR spectra were studied in a range of −40 to +40 ppm with tetramethylsilane as external standard while ^{13}C NMR experiments were conducted between −40 and +45 °C within a sweep range of 320 ppm downfield from the same standard. ^{31}P NMR spectra were recorded using 12-mm tubes and H_3PO_4 as external standard. The sweeps in this case were extended up to 400 ppm downfield from the standard.
(31) The term "cluster breathing" for the scrambling of this rhodium skeleton was suggested to us by Professor Paolo Chini.
(32) C. Brown, B. T. Heaton, P. Chini, A. Fumagalli, and G. Longoni, *J. Chem. Soc., Chem. Commun.*, 309 (1977).
(33) B. F. G. Johnson, *J. Chem. Soc., Chem. Commun.*, 703 (1973).
(34) The noble gas rule requires a number of electrons for $[Rh_9P(CO)_{21}]^{2-}$, $N_3 = 18N_1 - 2N_2$, of 122 = (18 × 9) − (2 × 20) = 162 − 40, but electron counting for this anion shows a number of total electrons of 130 = (9 × 9) + (2 × 21) + (1 × 5) + 2. Thus, it is concluded that the anion does not follow the noble gas rule. Similar calculation following Wade's rules, $N_3 = 14N_1 + \chi$,[20] 130 = (14 × 9) + χ, results in χ = 4, as required based on these rules for a nido cluster. The open-square basal face present on the anion structure (vide supra) is thus in agreement with Wade's rules predictions.

Contribution from the Department of Chemistry, University of Notre Dame, Notre Dame, Indiana 46556

Structural Characterization of the Hydrogen-Bridged Heterobimetallic Complex $(\eta^5\text{-}C_5H_5)_2(CO)Nb(\mu\text{-}H)Fe(CO)_4$

KWAI SAM WONG, W. ROBERT SCHEIDT,* and JAY A. LABINGER*

Received July 7, 1978

The structure of the product of the reaction of $(\eta^5\text{-}C_5H_5)_2NbH_3$ with $Fe(CO)_5$, $(\eta^5\text{-}C_5H_5)_2(CO)Nb(\mu\text{-}H)Fe(CO)_4$, has been determined by X-ray diffraction techniques. Crystals are monoclinic, space group $P2_1/c$, with cell parameters a = 7.835 (3) Å, b = 13.508 (2) Å, c = 15.165 (2) Å, β = 97.05 (2)°, and Z = 4. The structure was refined to R = 0.033 and R_w = 0.042 for 3063 unique observed data. The molecule contains a triangular Nb–H–Fe group with parameters Nb–Fe = 3.324 (1) Å, Nb–H = 1.91 (3) Å, H–Fe = 1.61 (3) Å, and Nb–H–Fe = 141 (2)°. The geometry about Nb is typical for $(\eta^5\text{-}C_5H_5)_2MX_n$ compounds, with a ring bending angle of 136.3°. The geometry about Fe is a nearly regular trigonal bipyramid (neglecting the bridging hydrogen) with the Nb atom in an axial position. NMR studies suggest a possibly different structure in solution.

Introduction

During the course of an investigation into the potential role of early transition-metal hydride complexes in catalytic CO reduction,[1] a new complex was isolated from the reaction of Cp_2NbH_3 (Cp = η^5-C_5H_5) and $Fe(CO)_5$. Since the analytical, spectroscopic, and chemical properties of this species did not permit complete and unequivocal characterization, a single-crystal X-ray structural determination was undertaken. A brief description of this study appeared in an earlier preliminary communication.[1]

Experimental Section

Synthesis and Characterization. All reactions and manipulations were carried out under inert atmosphere using standard techniques.[2] Infrared spectra were obtained on Perkin-Elmer Infracord and 457 instruments, ^1H and ^{13}C NMR spectra were taken on Varian A-60 and XL-100 instruments, and mass spectra were recorded on an AEI-MS9 instrument. Cp_2NbCl_2 was prepared according to a published procedure;[3] commercially available $Fe(CO)_5$ was used without further purification; solvents were distilled from benzophenone ketyl under argon prior to use. Elemental analysis was performed by Spang Microanalytical Laboratory.

A benzene solution of Cp_2NbH_3 was prepared by reaction of Cp_2NbCl_2 with $LiAlH_4$ followed by hydrolysis, as previously described,[4] and standardized by quantitative NMR measurement. Addition of a slight excess of $Fe(CO)_5$ results in essentially quantitative (by NMR) conversion to a new complex, formulated as $Cp_2(CO)Nb(\mu\text{-}H)Fe(CO)_4$ (I), accompanied by evolution of 1 mol of H_2/mol of starting niobium complex (determined manometrically). Removal of solvent and

0020-1669/79/1318-0136$01.00/0